Characterization of pea composites and feasibility of heat-modulated meat analogs production

Bhuiyan, Md. Hafizur Rahman; Liu, Laura; Samaranayaka, Anusha; Ngadi, Michael

Publisher’s version / Version de l'éditeur:

https://doi.org/10.1016/j.foodchem.2024.141282

Food Chemistry, 463, P2, 2024-09-13

Food Chemistry 463 (2025) 141282

Contents lists available at ScienceDirect

Food Chemistry

journal homepage: www.elsevier.com/locate/foodchem

Characterization of pea composites and feasibility of heat-modulated meat analogs production

Md. Hafizur Rahman Bhuiyan [a,*], Laura Liu [a], Anusha Samaranayaka [b], Michael Ngadi [a,*]

[a] Department of Bioresource Engineering, McGill University, Sainte-Anne-de-Bellevue, Quebec H9X 3V9, Canada
[b] National Research Council Canada, 110 Gymnasium Place, Saskatoon, SK S7N 0W9, Canada

ARTICLE INFO

Keywords:
Protein composites
Particle
Functionality
Meat alternative
Characterization

ABSTRACT

This study aimed to characterize pea composites' functionalities and investigate the feasibility of pea composites-based heat modulated meat analog (MA) production. Pea composites (concentrate, flour) were used as the main source of plant-proteins in preparation of MA. Techno-functional, sensorial, microstructural, chemical, and thermal characteristics of pea composites as well as the prepared MAs were investigated. Results showed that, protein content and particles size significantly ($p < 0.05$) influenced the water holding capacity (0.94 g/g ± 0.03–1.17 g/g ± 0.08), oil holding capacity (1.08 g/g ± 0.02–1.32 g/g ± 0.04), foaming capacity (49.20 % ± 0.12–58.9 % ± 0.98), foam stability (63.15 % ± 0.21–71.82 % ± 0.68), emulsion stability (61.73 % ± 1.68–66.02 % ± 1.25), least gelation concentration (at pH 7: 8.02 % ± 0.91–18.02 % ± 0.21), and solubility (at pH 7:70.51 % ± 2.54–93.71 % ± 1.86) of studied pea composites; that subsequently influenced the formation of heat-modulated MAs. Color, stickiness, moldability, microstructure (surface plot, fractal dimension: 2.771 ± 0.006–2.884 ± 0.009, surface openings: 8.76 % ± 1.25‾33.24 % ± 1.28), thermal (denaturization temperature:103.41 °C ± 3.87–161.20 °C ± 1.35, enthalpy: 1085.10 J/g ± 115.42–1322.71 J/g ± 185.65), and chemical attributes of MAs were associated with the protein content (25.30 % ± 0.98–60.30 % ± 1.87) and particle size (d_{10}:2.30 μm ± 0.32–15.02 μm ± 1.35; d_{50}:6.30 μm ± 1.02–59.01 μm ± 2.35; d_{90}:15.11 μm ± 2.34–137.01 μm ± 15.21) of pea composites. MA formulated with pea flour showed better moldability and acceptability in comparison to pea concentrates. This study exposed the use of pea flour as a feasible option to produce heat modulated meat analogs.

1. Introduction

There is continuously increasing demand of animal-meat alternatives (Bhuiyan et al., 2024a; Hong et al., 2022; Mittal et al., 2023; Yuliarti et al., 2021). To meet consumer demand of animal-meat alternatives, the development of plant-proteins based meat analog (MA) is a rapidly growing industry (Bhuiyan et al., 2024a; Bhuiyan & Ngadi, 2024a; Yuliarti et al., 2023). In preparing plant-proteins based MA, the use of different ingredients (e.g., protein, water, fat, etc.) is a very common industrial practice (Bhuiyan et al., 2024a; Yuliarti et al., 2023).

In large scale industrial preparation of MAs, the use of most purified forms of protein composite (i.e., isolate, containing about 80–94 % protein) is a very common strategy (Bhuiyan et al., 2024a; Rodriguez & Beyrer, 2023; Yuliarti et al., 2021). In line with this, scientific literature relating protein isolates functionality in relation to different aspects of meat-analogs are available in literature. It could be highlighted that commercial price of protein composites largely associated with their protein percentage, wherein concentrate and flour fractions are economical choice (due to presence of low protein) over the isolate fraction. However, study relating to possible use of low-percentage protein containing composite (i.e., concentrate, flour) in the production of MA is not available yet. Furthermore, it has been pointed that non-protein residue (present in used protein composite) may have impact on the functionalities of their protein component (Xu et al., 2023). Hence, it could be hypothesized that presence of low-protein in concentrate and flour fractions (in other word, presence of other non-protein components) might have influence attributes of the formulated MAs, distinctively. However, the possibility and of impacts of low-protein containing composites (concentrate, flour) in preparing MA, is still unexplored.

At present the main processing technologies for the production of MA are extrusion, electrospinning, and shear cell technologies (Beniwal

* Corresponding authors.
E-mail addresses: md.bhuiyan@mail.mcgill.ca (Md.H.R. Bhuiyan), michael.ngadi@mcgill.ca (M. Ngadi).

https://doi.org/10.1016/j.foodchem.2024.141282
Received 2 June 2024; Received in revised form 3 September 2024; Accepted 11 September 2024
Available online 13 September 2024

et al., 2021; Bhuiyan et al., 2024a; Hu et al., 2023; Sha & Xiong, 2020; Woo et al., 2024; Xia et al., 2023). The major limitations of these technologies include high equipment costs, high energy/power requirements, needs of highly technical personnel, etc. (Hu et al., 2023; Ladha-Sabur et al., 2019). Hence, there is commercial interest in identifying less expensive, energy efficient, and low energy requiring methods for creating plant derived composites-based meat analogs (Bhuiyan et al., 2024a; Hu et al., 2023). To this context, heat-modulated (i.e., application/rejection of heat to form structure) MA formation is an innovative approach that has been reported in most recent literature (Bhuiyan et al., 2024a; Bhuiyan & Ngadi, 2023a; Yuliarti et al., 2021). In literature, heat-rejection based structure formation in MAs have been reported (Yuliarti et al., 2021; Yuliarti et al., 2023). However, understanding of the mechanisms of heat-application based MA formation is prerequisite before its large-scale commercial application. Furthermore, how heat-modulated MA formation is impacted by the types of protein composites (concentrate, flour), is still unknown.

Price and functionality of raw ingredients are directly involved with quality and production cost of the final products (Rodriguez & Beyrer, 2023; Webb et al., 2023). It could be hypothesized that plant-composites' (protein) functionalities would play crucial role in developing plant-ingredient based MA, and the use of comparatively low-price ingredients will be in favor of lowering the production cost of meat analogs. The relationship between plant proteins functionality and development of MA by employing novel heat-modulated (application of heat) method, is still unexplored. Considering the above-mentioned issues and limitations, this study characterizes pea composites functionalities and investigated the feasibility of pea composites-based heat modulated meat analogs production. Overall, the thermo-functional, mechanical, sensorial, chemical, and structural characteristics of plant protein composites (pea concentrate, pea flour) as well as characteristics of these composites-based heat modulated MAs were thoroughly investigated.

2. Materials and methodology

2.1. Materials

In this study, pea composites (concentrate, flour) were used as the main source of plant-proteins in preparation of the meat analogs. Pea composites (pea protein concentrate, pea flour) were procured (dry fractionated) from the Department of Bioresource Engineering, McGill University, Canada. In this study, pea concentrates were labeled as PC1, PC2, PC3 & PC4 (based on protein content); and pea flour was labeled as PF. Wheat gluten (WG) was supplied by Sigma-Aldrich Co. (Ontario, Canada). Canola oil (CO) was procured from local grocery shop at Montreal, Canada.

2.2. Moisture and protein determination

Pea composites were evaluated for moisture and protein content as detailed in relevant studies (Bhuiyan et al., 2024a; Eze et al., 2024; Chiang et al., 2019; Yuliarti et al., 2021).

To determine moisture content, samples were freeze dried in a freeze-dryer (Modulyod-115; Thermo Savant, Holbrook, NY, U.S.A.) at −50 °C and 250 mbar for 48 h and then transferred into a desiccator to equilibrate for 30 min. Weight of the sample before and after drying was measured and moisture content was calculated based on weight difference (Bhuiyan et al., 2024a; Eze et al., 2024).

Protein content was determined by estimating total nitrogen via Dumas method by using a dumas nitrogen analyzer (NDA 701, Velp Scientifica, Usmate, Italy). The nitrogen content was multiplied by 6.25 for pea composites (Yuliarti et al., 2021; Chiang et al., 2019).

2.3. Particle size distribution and bulk density

Particle size distribution were assessed by the methods of Webb et al. (2023). In brief: particle size distribution was determined using an Air Jet Sieve e200LS (Hosokawa Alpine Group, Augsburg, Germany). A 100 g sample was placed on the smallest sieve with a negative pressure of 3400 Pa applied to the underside of the sieve to remove and transport particles finer than the screen into a collecting jar. The weight of the overs or remains on the screen were transferred to the next largest sieve and the process was repeated with progressively higher screen sizes until all material passed through. Sieves with 32, 53, 75, 106, 125, 150, 180, 212, 250 and 300 μm were used. The particle size distribution (d_{10}; d_{50}; d_{90}) value were reported as μm.

Bulk density was determined as per method of (Hong et al., 2022), with slight modification. Pea composite was filled in a graduated cylinder with gentle tapping twice to eliminate the interspace of the crumbles. Volume and weight were recorded, and the bulk density was calculated as weight per *v*olume (g/ml).

2.4. Water and oil absorption capacity

Water and oil absorption of pea composites were measured by the modified methods of Deriu et al. (2022) and (Eze et al., 2024). Samples (2.0 g) were dispersed in 20 ml of distilled water or vegetable oil, placed in reweighed 50 ml centrifuge tubes. The dispersions were vortexed on high speed for 30 s after which they were held at room temperature for 30 min. Followed by centrifugation for 30 min at 3000 rpm. The supernatant was decanted, and the tubes were inverted and held in that position for 25 min, to further drain off excess moisture or oil. Final weight of the sediment was recorded. The water and oil absorption capacities were expressed as g water or oil/ g of flour sample (g/g, dry basis).

2.5. Foaming capacity and stability

Foaming capacity and stability of samples were determined by slightly modifying the methods of Abebe et al. (2015) and (Eze et al., 2024). The 50 ml of a 3 % (*w*/*v*) dispersion of pea composite sample in distilled water were homogenized using homogenizer (Ultra Turrax, Wilmington, USA), at high setting for 3 min. The blend was immediately transferred into a graduated cylinder and the homogenizer cup was rinsed with 10 ml distilled water, which were then added to the graduated cylinder. The volume was recorded before and after whipping and measured as the % of volume increase due to whipping. The foaming activity was expressed as % of volume increase. Foam stability was recorded as volume changes in the graduated cylinder after 30 min of standing (Eze et al., 2024).

2.6. Emulsion activity and stability

Emulsifying properties were determined according to the methods of (Eze et al., 2024) and Arteaga et al. (2020) with slight modification. Pea composites (3.5 g) was homogenized for 30 s in 50 ml water in a homogenizer (Ultra Turrax, Wilmington, USA) at high setting. Vegetable oil (25 ml) was added, and the mixture was homogenized again for 30 s. Then, another 25 ml of vegetable oil was added, and the mixture was homogenized on high speed for 90 s. The emulsion was divided evenly into two 50 ml centrifuge tubes and centrifuged at 1100*g* for 5 min. Emulsifying activity was calculated by dividing the volume of the emulsified layer by the volume of emulsion before centrifugation.

Emulsion stability was determined using the samples prepared for measurement of emulsifying activity. They were heated for 15 min at 85 °C, cooled and centrifuged again at 1100*g* for 5 min. The emulsion stability was expressed as the percent (%) of emulsifying activity remaining after heating.

2.7. Least gelation concentration

Sample solutions were prepared in 5 ml tubes containing suspensions of 2, 4, 6, 8, 10, 12, 14, 16, 18 and 20 % (*w/v*) of pea composites. The samples were heated in a water bath at 95 °C for 30 min, cooled to room temperature for 1 h and left overnight at 4 °C before the tubes were inverted. The least gelation concentration (LGC) is the concentration above which samples did not fall down or slip when the test tubes were inverted (Eze et al., 2024).

2.8. Protein solubility

The dispersion for each sample was stirred for 30 min and adjusted to pH 3 and 7.0, with O.1 M HCl or NaOH solution. The suspension was shaken for 1 h, where the solution was centrifugated at 10000 rpm for 10 mins using the approach described by Morr et al. (1985). The Biuret method was used to estimate soluble protein. Soluble protein content was analyzed photometrically at 550 nm using bovine serum albumin (BSA) as the standard for calibration. The soluble protein content was expressed as the %protein content present in the sample.

2.9. Color measurement

Color parameters of samples were measured based on CIE1976 system by a colorimeter (Minolta Spectrophotometer CM-3500d, Japan). The color difference (ΔE) was estimated based on Lab values as detailed by (Bhuiyan & Ngadi, 2023a).

2.10. Meat analogs

Meat-analog (MA) was formulated with pea composites (concentrate/flour), wheat gluten (WG), distilled water (DW) and canola oil (CO). Fig. 1 depicts the step of meat-analog preparation, in brief: firstly, wheat gluten was mixed with canola oil. Then the pea composite was added to the mixture. Finally, distilled water was added and mixed thoroughly. Respective proportion (g) of the ingredients for MA preparation were pea composites: wheat gluten: canola oil: water = 11: 6: 7.5:15 (weight basis). After preparing the dough of these ingredients, the prepared dough was used to fill the rectangular sized cavity of the silicon mold and cover with aluminum foil. Then the mold filled with the dough mix was heated (at 70 °C for 30 min) in water bath. Then the mold was allowed to cool to room temperature, and gently pressure was applied at the back of the silicon mold to bring out the restructured MA.

2.11. Differential scanning calorimetry (DSC)

Differential scanning calorimetry of the pea samples were performed by using a differential scanning calorimeter (DSC Q250, TA Instrument, New Castle, DE, USA). In brief: around 6–10 mg of pea sample (powder form) was placed in the DSC sample pan, a lid was attached, and a mechanical device was used to hermitically sealed them. For some samples the pea powder was mixed with distilled water where the mixing ratio of power and water was equal (i.e., mg to μl). However, one sample holder with a lid (but without crust sample) was used as a reference pan. In DSC measurement chamber: sample was rapidly cooled to −40 °C at a cooling rate of 10 °C/min, held isothermally for 2 min, and then heated to +250 °C at a rate of 5 °C/min. DSC data were recorded and analyzed using DSC-Trios ver.5.1.1 software (TA Instrument, New Castle, DE, USA).

2.12. Scanning electron microscopy (SEM)

The SEM image were obtained by using a scanning electron microscope (Hitachi TM3000, Japan). To obtain SEM image of composites (powder form), the pea composites were carefully placed over the black carbon tape on SEM sample holder, and excess powders were blown off from the sample holder. To obtain SEM image of the formulated model foods surface, following the method of Bhuiyan and Ngadi (2024a, 2024b) a small cut, rectangular shaped, defatted sample of about 10 × 10 × 5 mm was used to obtain SEM image of the samples surface. SEM images of powder samples were acquired at a magnification of ×600 and magnification of ×80 was used to obtain SEM image of model. Acquired images were analyzed by public domain image processing software (Image J, National Institutes of health, USA).

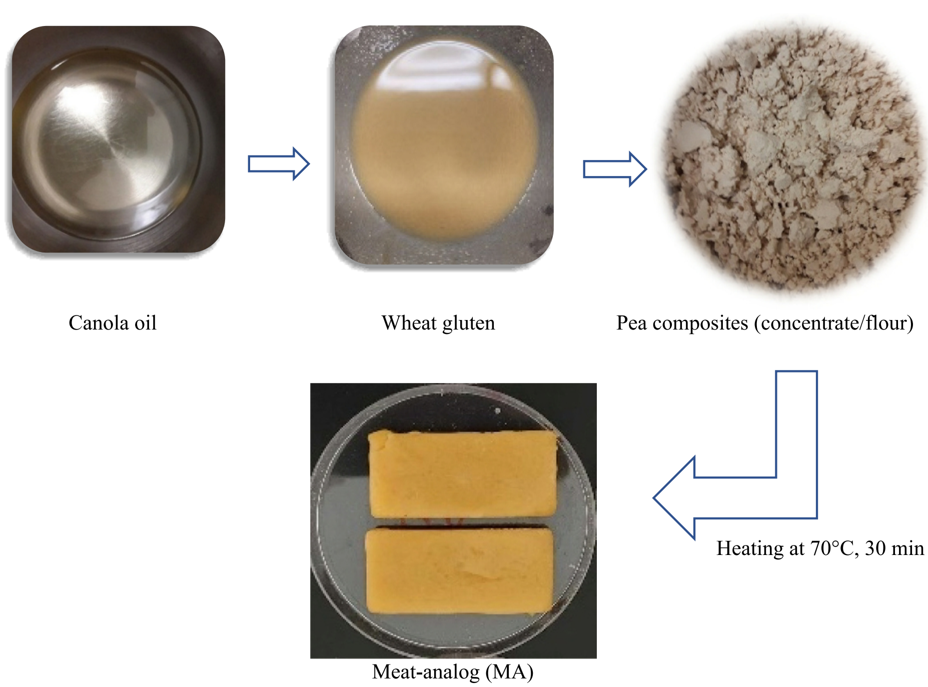

Fig. 1. Preparation steps of pea protein composites-based meat analogs.

2.13. ATR-FTIR spectroscopy

FTIR spectra of samples were recorded by an ATR-FTIR spectrometer (Thermo Scientific Nicolet iS5 FTIR, Thermo Fisher Scientific, USA). The methods of Bhuiyan & Ngadi (2024a, 2023a) were followed in performing FTIR Spectroscopy. The FTIR spectra were collected over the wavenumber range of 4000–600 cm^{-1} by co-adding 32 scans and at resolution of 4 cm^{-1}. All spectra were normalized against background of air spectrum. Absorption area under the IR spectral ranges between 1130 and 1200, 1400–1500, 1700–1800, and 2800–3000 cm^{-1} were calculated and their summed value was reported as fat response (FR). Absorption area in IR spectra within 3000–3700 cm^{-1} range were considered as moisture response (MR). The IR absorption band within the range between 1700 and 1590 cm^{-1} were considered as protein response (PR). The absorption within the ranges of 1590–1475, 1300–1175 and 1200–900 cm^{-1} were summed and reported as carbohydrate response (CR).

2.14. Statistical analysis

All experimental data obtained from at least triplicate of samples, mean ± SD (standard deviation) was reported. Tukey's honestly significant difference (HSD) was used in reporting significant ($p < 0.05$) difference among mean values. Statistical analysis is performed by licensed statistical software (JMP 14.1v, SAS Institute Inc., Cary, NC, USA).

3. Results and discussion

3.1. Techno-functional properties

Table 1 summarizes the techno-functional properties of pea composites (concentrate, flour). Protein content of the studied pea protein concentrate (PC) were ranged between 46.71 % ± 1.12 and 60.30 % ±1.87. Protein content (25.30 % ± 1.98) of pea flour (PF) was significantly lower than pea protein concentrates. Generally, the most purified form of protein composites contains higher protein than their less purified form (Rodriguez & Beyrer, 2023). Protein content ranges between 52.4 and 56.4 % has been reported for chickpea concentrates (Yaputri et al., 2023), and ranges between 23.8 and 46.8 % has been reported for lentils composites (Xu et al., 2023).

Moisture content of the dry pea composites were ranged between 5.87 % ± 0.54 and 9.17 % ± 1.13, where a slightly higher moisture was determined for PF sample. This difference in moisture could be attribute to their distinctive production process as well as distinctive matrix structure, as matrix's structure could influence the chemical profile of biomaterials (Bhuiyan et al., 2024b). However, moisture content ranged between 5.8 and 8.1 % has been reported for plant-protein enriched composites (Hong et al., 2022).

The starch content of PCs (ranged between 1.92 % ± 0.67 and 5.47 % ± 0.32) were significantly lower than (45.30 % ± 2.15) the starch content of PF. Insoluble fiber content of PCs was ranged between 5.76 % ± 1.02 and 16.30 % ± 1.02 whereas insoluble fiber content of the PF was 6.21 % ± 1.34. Higher starch and insoluble fiber content of PCs in comparison to PF be attribute to their distinctive production process.

Particle size distribution ($d_{10,}$ d_{50} & d_{90} value) indicate that there were significant ($p < 0.05$) differences among the pea composites. Particle size (μm) of the PF were substantially larger in size than the particle of PCs. It has been reported that particle size of plant-proteins can vary based on industrial processing which can cause the increased denaturation and aggregation of hydrophobic regions (Webb et al., 2023).

Bulk density (BD) of pea protein concentrates (ranged between 0.51 g/ml ±0.05 to 0.59 g/ml ±0.08) were significantly lower than the BD of pea flour (0.77 g/ml ± 0.11). These BD values are in close similarity with the study of (Hong et al., 2022; Webb et al., 2023). However, the variation in bulk density of pea composites could be attribute to their variation in moisture content and size of the particles.

Table 1
Techno-functional properties of pea composites.

Attribute	PC1	PC2	PC3	PC4	PF
Protein (%)	46.72 ± 1.12^{c}	52.61 ± 1.22^{b}	58.80 ± 1.03^{a}	60.30 ± 1.87^{a}	25.30 ± 0.98^{d}
Moisture (%)	8.38 ± 1.10^{a}	6.57 ± 1.05^{ab}	5.87 ± 0.54^{b}	7.88 ± 0.98^{a}	9.17 ± 1.13^{a}
Total starch (%)	5.47 ± 0.32^{b}	5.23 ± 0.54^{b}	1.92 ± 0.67^{c}	3.45 ± 0.55^{bc}	45.30 ± 2.15^{a}
Insoluble fiber (%)	16.30 ± 1.02^{a}	12.5 ± 0.98^{a}	13.09 ± 1.21^{a}	5.76 ± 1.02^{b}	6.21 ± 1.34^{b}
Soluble fiber (%)	<0.10 ± 0.03^{b}	1.12 ± 0.08^{a}	1.03 ± 0.11^{a}	<0.10 ± 0.01^{b}	0.90 ± 0.08^{a}
Particle size distribution, d_{10} (μm)	2.30 ± 0.32^{b}	2.41 ± 0.18^{b}	2.31 ± 0.21^{b}	2.11 ± 0.14^{b}	15.02 ± 1.35^{a}
Particle size distribution, d_{50} (μm)	7.90 ± 1.22^{b}	7.20 ± 1.40^{b}	6.91 ± 1.34^{b}	6.30 ± 1.02^{b}	59.01 ± 2.35^{a}
Particle size distribution, d_{90} (μm)	21.81 ± 2.27^{b}	18.71 ± 2.32^{b}	17.02 ± 1.58^{b}	15.11 ± 2.34^{b}	137.01 ± 15.21^{a}
Bulk density, BD (g/ml)	0.53 ± 0.05^{b}	0.59 ± 0.08^{b}	0.57 ± 0.06^{b}	0.51 ± 0.05^{b}	0.77 ± 0.11^{a}
Water holding capacity, WHC (g/g)	1.06 ± 0.01^{a}	0.98 ± 0.02^{a}	1.02 ± 0.02^{a}	1.17 ± 0.08^{a}	0.94 ± 0.03 ^{b}
Oil holding capacity, OHC (g/g)	1.11 ± 0.02^{bc}	1.18 ± 0.03^{ab}	1.23 ± 0.01^{a}	1.32 ± 0.04^{a}	1.08 ± 0.02^{c}
Foaming capacity, FC (%)	52.6 ± 0.02^{b}	54.21 ± 0.03^{b}	58.70 ± 0.44^{a}	58.9 ± 0.98^{a}	49.20 ± 0.12^{c}
Foam stability, FS (30 min)	67.9 ± 0.32^{bc}	69.70 ± 0.74^{a}	70.81 ± 0.54^{a}	71.8 ± 0.68^{a}	63.15 ± 0.21^{c}
Emulsion stability, ES (%)	66.0 ± 1.25^{a}	65.51 ± 1.65^{a}	62.70 ± 1.48^{a}	61.7 ± 1.68^{a}	–
Least gelation concentration, LGC (%) at pH 7	13.00 ± 0.21^{b}	11.11 ± 0.68^{bc}	8.02 ± 0.91^{c}	14.01 ± 0.08^{b}	18.02 ± 0.21^{a}
Least gelation concentration, LGC (%) at pH 3	12.02 ± 0.98^{ab}	11.03 ± 0.35^{b}	10.01 ± 0.21^{b}	9.01 ± 0.14^{b}	14.02 ± 1.21^{a}
Solubility, PS (%) at pH 7, with 0.1 M Phosphate buffer	90.21 ± 1.85^{a}	90.83 ± 1.35^{a}	91.50 ± 1.77^{a}	93.71 ± 1.86^{a}	70.51 ± 2.54^{b}
Solubility, PS (%) at pH 3, with 0.1 M Citrate buffer	27.3 ± 1.58^{a}	27.8 ± 1.86^{a}	29.5 ± 1.23^{a}	27.52 ± 1.76^{a}	–

Values are shown as mean ± standard deviation. Lower case letters (a-c) represent significant ($p < 0.05$) difference among pea composites. PC and PF represent pea protein concentrate and pea flour, respectively.

Water holding capacity (WHC) describes the capability of proteins to hold water molecules against gravity through hydrogen bonds and are trapped by the hydroxyl groups of carbohydrates and proteins (Cruz-Solorio et al., 2014). WHC of pea protein concentrates (ranged between 0.98 g/g ± 0.02 and 1.17 g/g ± 0.08) were significantly higher than (0.94 g/g ± 0.03) pea flour. The dissimilarity in WHC reflects that there was variation in the hydrophilic content of amino acids, conformation, type, and quality of protein as well as other non-protein components in the pea composites. It is notable that in compared to the coarser flours, the finer flours generally exhibit higher ability to absorb/retain more water due to their larger surface area and presence of more damaged particle structures (Maskus et al., 2016).

Oil holding capacity (OHC) describes the quantity of oil absorbed per unit gram of protein. It is an important techno-functional property of flours and proteins as it influences mouthfeel, product yield, flavor, and texture (Wang et al., 2020). The manufacturers of meat analogues, baked goods, doughnuts, meat extenders, etc. used it as a quality index (Ma, 2020). The OHC of pea protein concentrates (ranged between 1.11 g/g ± 0.02 and 1.32 g/g ± 0.04) were significantly ($p < 0.05$) higher than the oil holding capacity (1.08 g/g ± 0.02) of pea flour. Ika et al. (2020) obtained a varied oil holding capacity (ranged between 0.27 and 2.86) for cowpea concentrates. However, higher OHC of pea protein concentrates could of the consequences of the physical activity of oil entrapment due to the protein's hydrophobicity. In addition, structure of protein matrix, form of lipids, as well as organization and stability of the lipids might have influences OHC of pea composites. The observed variation in OHC of different pea composites could be due to the differences in the non-polar amino acids, that might bind the lipid hydrocarbon chains during oil absorption.

Foaming capacity (FC) describes the protein's water solubility and water absorptivity at the interface, as the air bubbles are surrounded by a protective membrane to stabilize the air bubble films (Boukid et al., 2021). FC of pea protein concentrates (ranged between 52.6 % ± 0.02 and 58.9 % ± 0.98) were significantly higher than (49.20 % ± 0.12) pea flour. FC ranged between 16.4 and 32.8 % has been reported for lentils and beans (Xu et al., 2023). However, higher FC of the studied PCs could be due to the presence of higher amount of proteins in studied pea protein concentrates. It is important to mention, to obtain high quality emulsions and foam forming capacities, more protein-protein interactions are important for the interfacial membrane formation at the oil-water and air-water interfaces (Aluko et al., 2009). In literature, in comparison to the foaming capacity (25.30 %) of pigeon pea flour, higher foaming capacity (ranged between 33.23 and 35.37 %) has been reported for pigeon pea concentrates and isolates (Adenekan et al., 2018). Foaming capacity in the ranges between 18 and 45.33 % has been reported for soybean concentrates (Ika et al., 2020). However, variation in FC of the studied pea composites suggests that the protein's water solubility and water absorptivity varied based on the composites type and varieties. However, non-protein components such as carbohydrates could also influence the foaming capacity of legume-based proteins (Sreerama et al., 2012).

Foam stability (FS) is a critical factor in protein and food processing industry. FS (30 min) of pea protein concentrates (ranged between 67.91 % ± 0.32 and 71.82 % ± 0.68) were significantly higher than the stability (63.15 % ± 0.21) of pea flour. In literature, foam stability ranged between 52.3 and 55.7 % has been reported for pigeon pea isolates (Adenekan et al., 2018).

Emulsion stability (ES) of the studied PCs were very similar and ranged between 61.73 % ± 1.68 and 66.02 % ± 1.25. Du et al. (2014) reported emulsion stability of 61.14–92.20 % for legume flours. Ivanova et al. (2014) reported a varied ES between 45.85 and 60.88 % for protein isolate of sunflower meals. It could be mentioned that a high quantity of hydrophobic surface area may leads to more flexibility in protein structure which can improve the emulsion stability through interfacial action (Sahin & Sumnu, 2006).

The least gelation concentration (LGC) is used to determine the heat-gelling (i.e., ability of a protein to form a three-dimensional network through its denaturation and aggregation) properties of proteins (Webb et al., 2023). The LGC (at pH 7) of pea protein concentrates (ranged between 8.02 % ± 0.91 and 14.01 % ± 0.08) were significantly lower than the pea flour (18.02 % ± 0.21). Variations in the amount of flour constituents such as protein, carbohydrate and lipids may have affected the LGC. However, the least gelation concentration (at pH 3) of pea composites were ranged between 9.01 % ± 0.14 and 14.02 % ± 1.21.

Protein solubility (PS) measures the degree of denaturation/permanent precipitation and aggregation, that could occur during the isolation/extraction process. The PS (at pH 7) of pea protein concentrates (ranged between 90.21 % ± 1.85 and 93.71 % ± 1.86) were significantly higher than PS of pea flour (70.51 % ± 2.54). Protein solubility (at pH 7) within the range between 70.7 and 84.3 % has been reported for chickpea composites (Yaputri et al., 2023). A solubility value ranged between 27.7 and 82.0 % has been reported for lentils and beans (Xu et al., 2023). The protein solubility (at pH 3) of pea protein concentrates were ranged between 27.31 % ± 1.58 and 29.5 % ± 1.23. A protein solubility of chickpea composites at pH 3 were reported within the range between 12. And 23.8 % (Yaputri et al., 2023). Adenekan et al. (2018) reported a protein solubility value of 12.1 % for pigeon pea flour, and protein solubility value of 90.7–97.13 % for pigeon pea isolates. However, in this study PS showed a linear correlation with the percentage of protein. Similar observation has been reported for faba bean and soybean protein isolates (Karaca et al., 2011). The variation in PS of the studied pea composites could be due to the variation in hydrophobicity and surface composition of protein molecules of the studied pea composites (Shanthakumar et al., 2022).

3.2. Sensorial characteristics

Table 2 summarizes the sensorial attributes of pea composites and formulated meat-analogs. The lightness (L value) of studied PC and PF ranged between 90.80 ± 1.74 and 94.10 ± 1.87. The slight greenness (−a* value) color tone of the sampled between −0.42 ± 0.18 and − 1.61 ± 0.06. The yellowness (+b* value) of studied PCs and PF ranged between 16.11 ± 1.22 and 27.52 ± 1.21. The L value within a range between 85.2 and 92.2, a* value in the ranges between −1.21 and − 0.62, and b value in the ranges between 9.05 and 13.7 have been reported for the chick pea composites (Yaputri et al., 2023). However, differences in color attributes among the studied pea composites (in powder form) were substantial. The overall color differences can be visually evident from the camera image of the powder samples.

The lightness (L value) of pea composites based formulated MAs were ranged between 59.50 ± 1.32 and 68.12 ± 1.04. This lightness value of MAs is substantially lower than corresponding powder of the pea composites. This could be attributed to the presence of water in formulated MA, which was almost absent in the dry powder of pea composites. In comparison to slight greenness (−a* value) color tone of pea composites powder, the redness (+a* value) color tone was observed in formulated MAs where the value ranged between 0.40 ± 0.12 and 8.31 ± 0.65. The changes in color (from greenness to yellowness) could be associated with the formation of color compounds via chemical interactions (browning, Maillard reaction, gelatinization, etc.) within the formulated meat analogs. The yellowness (+b* value) color tone of the formulated MAs were ranged between 30.90 ± 1.21 and 38.70 ± 0.98. The yellowness color tone of MA was substantially higher than powder form of the corresponding pea composites. This increase in yellowness in MA could be associated with the presence of canola oil in formulated MA, as color of the used oil was yellowish. The total color difference (ΔE) value ranged between 28.11 ± 1.58 and 47.60 ± 1.32. It is noticeable that highest ΔE value was estimated for the PC4 followed by PC3, PC2 and PC1. Whereas lowest ΔE value was estimated for the PF sample. Higher ΔE value represents higher degree of color changes (powder vs meat-analog) in studied matrix (Bhuiyan & Ngadi, 2023a). Highest extent of color changes for PC4 could be associated with its higher protein content. It could be mentioned that Maillard reaction favors color changes in food matrix, and this reaction requires amino acids (i.e., protein entities) which was abundant in PC4 sample.

Sensorial textural feeling is very crucial for any food matrix. The stickiness and moldability of the pea composites were greatly impacted by the type of composites. Higher stickiness was assessed in PC4 samples followed by PC3, PC2 and PC1. The stickiness of these pea concentrates could be linked with their higher protein content, as protein supports higher viscoelastic nature in food matrix by forming strong 3D network structure (Xue & Ngadi, 2006). However, higher moldability and acceptability were observed for the PF composite. From large scale production point of view, it could be suggested that the formulation of MA needs to be optimized on the basis of the ingredient's functionality.

3.3. Microstructural characteristics

Table 3 depicts the scanning electron microscopy (SEM) images and assessed structural attributes of both the pea composites and formulated meat-analogs. It is visually evident that particle size of pea composites varied greatly, wherein the particle size of PF was too much larger than pea concentrates (PC1, PC2, PC3 & PC4). This observation is in agreement with the particle size distribution as assessed by particle size

Table 2
Sensorial characteristics of pea composites and meat-analogs.

Sample type	Attribute	PC1	PC2	PC3	PC4	PF
Dry powder	L value	94.10 ± 1.87^{a}	93.50 ± 2.02^{a}	92.80 ± 1.88^{a}	91.30 ± 2.35^{a}	90.80 ± 1.74^{a}
	a* value	-1.61 ± 0.06^{a}	-1.41 ± 0.11^{a}	-0.72 ± 0.15^{b}	-0.42 ± 0.18^{b}	-0.81 ± 0.32^{b}
	b* value	19.10 ± 0.98^{b}	16.11 ± 1.22^{b}	17.60 ± 1.04^{b}	21.41 ± 1.35^{ab}	27.52 ± 1.21^{a}
	Camera image					
Meat-analog	L value	64.50 ± 1.03^{ab}	59.30 ± 0.98^{b}	58.80 ± 1.14^{b}	59.50 ± 1.32^{b}	68.12 ± 1.04^{a}
	a* value	2.31 ± 0.32^{b}	4.41 ± 0.12^{ab}	7.21 ± 0.35^{a}	8.31 ± 0.65^{a}	0.40 ± 0.12^{c}
	b* value	33.50 ± 0.98^{ab}	30.90 ± 1.21^{b}	32.81 ± 0.65^{b}	31.50 ± 0.08^{b}	38.70 ± 0.98^{a}
	ΔE value	37.21 ± 1.95^{b}	38.82 ± 1.86^{b}	42.22 ± 1.54^{ab}	47.60 ± 1.32^{a}	28.11 ± 1.58^{c}
	Camera image					
	Moldability	Good	Moderate	Not good	Not good	Very good
	Stickiness	Low	Moderate	High	Too high	Low
	Acceptability	Good	Moderate	Very low	–	High

Values are shown as mean ± standard deviation. Lower-case letters (a-c) represent significant ($p < 0.05$) difference among means (within row). PC and PF represent pea protein concentrate and pea flour, respectively.

analyzer (Table 1). Among the pea protein concentrates (PC1, PC2, PC3 & PC4) a marginal variation in particle size was noticed. However, it is noteworthy that most of the particles of PF sample was bigger while some particles were comparatively smaller in size. In contrast, most of the particle of pea concentrates were small in size while some particle was slightly large. The observed differences in particle size of studied pea composites might be the resultant effect of their respective processing treatments/operations. The difference in particle size of dry powder might play role matrix (by influencing inter particle network) in developing food products having different structural characteristics.

The micrograph of pea composites-based MA depicts clear differentiation in their microstructure. Compact microstructure was observed for the MA prepared with PC4 followed by PC3 and PC2. The microstructure of PC1 and PF based meat-analogs were comparatively less compact. This observed difference in MAs microstructure could be linked with their particle size and protein content, and could be understand as such: the particle size of PC4 was very smaller in comparison to PF. Smaller size particles were able to come in close contact to each other's and were easily fused together (under processing treatment), that results into a compact MA structure. Whereas, under same processing treatment the larger size particles of PF weren't very strongly attached to each other's (due to lower degree of impacts of the processing treatment), hence, a less compact microstructure was observed. It is noteworthy that protein content of PC4 was significantly ($p < 0.05$) higher than the protein content of PF samples. It has been reported earlier, protein possess the good film/network forming ability (Xue & Ngadi, 2006) and this attribute might had favored the formation of compact microstructure in PC4 based meat-analogs. It could be mentioned that the higher protein content may undergo a higher degree of protein cross-linking and may form strong structures (Hong et al., 2022).

Surface plot depicts roughness/smoothness of the formulated MAs. It is visually evident that the surface of PF based meat-analog was substantially rough in comparison to the surface of PCs based meat-analogs. In comparison to estimated fractal dimension value (2.927 ± 0.005) of PF based meat-analog sample, significantly lower fractal dimension values (ranged between 2.884 ± 0.009 and 2.771 ± 0.006) of the PCs corroborates the lower surface roughness (i.e., higher smoothness). Higher surface smoothness of pea protein concentrate based MA could be associated with their higher protein content, as protein possess good film forming capacity. In literature (Bhuiyan & Ngadi, 2023a; Bhuiyan & Ngadi, 2024a) it has been highlighted that the surface roughness of protein based processed food matrix greatly depends on formulation of the matrix. In this study, protein content of PF was significantly ($p < 0.05$) lower than the PCs and higher roughness was observed in PF based formulate meat-analogs. In addition to roughness, the estimated surface opening (SO) was also impacted by the type of pea composites. In comparison to the SO (ranged between 28.73 % ± 1.33–8.76 % ± 1.25) of pea protein concentrate based meat-analogs, significantly higher SO (33.24 % ± 1.28) were estimated for PF based meat-analogs. Higher SO value indicates lower interconnected matrix (as seen in SEM micrograph). Overall, the attributes of pea flour as well as PF based formulated meat-analog were more closely reassemble to PC1. The higher similarity in attributes of PF and PC1 could be due to closeness in their physicochemical and structural nature.

3.4. Thermal characteristics

Fig. 2 depicts differential scanning calorimetry (DSC) curves and Table 4 summarizes thermal properties of pea composites and formulated MAs. The DSC curve showed that the pea composites (dry powder form) exhibited two distinctive endothermic peaks (within the temperature range of −30 °C to 175 °C). Rodriguez and Beyrer (2023) reported similar observation for leguminous protein composites. However, the first peak was very small in height and size, and were appeared at low temperature range between 48.10 °C ± 1.02 and 51.20 °C ± 1.33. This lower temperature value associated with the small peak could be associated to the starch gelatinization process (i.e., heat treatment of starch and water generally causes the starch granules to expand where water is gradually absorbed in an irreversible manner, and that results into a viscous and transparent texture of the system). For different types of lentil flours, Eze et al. (2024) reported similar small peak in the temperature ranges between 60 °C and 70 °C. However, the second broad peak was at a higher temperature with an onset temperature range between 70.21 °C ± 1.14 and 97.31 °C ± 1.21. This temperature range could be associated with the denaturization (i.e., protein loses the folded structure present in their native state) of the studied pea composites. For leguminous protein composites, Rodriguez and Beyrer (2023) reported intense peak temperature at around 77.8 °C. A denaturization

Table 3
Morphological characteristics of pea composites and meat-analogs.

Sample type	Attribute	PC1	PC2	PC3	PC4	PF
Dry powder	Micrograph M: 500×	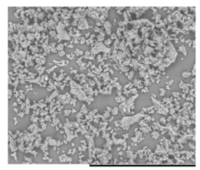	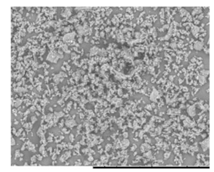	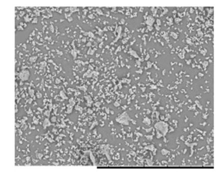	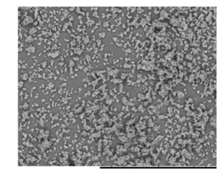	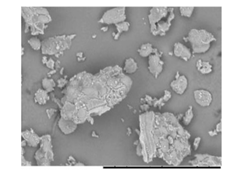
Meat-analog	Micrograph M: 100×	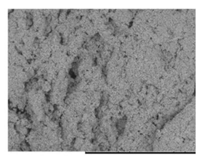	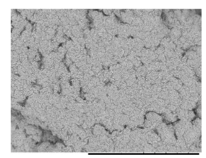	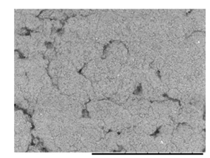	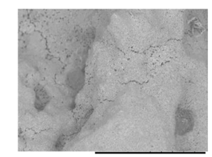	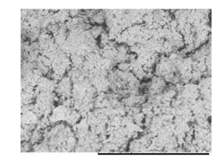
	Surface plot	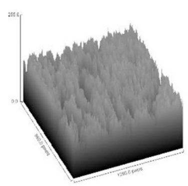	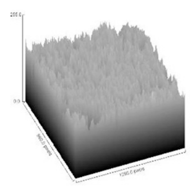	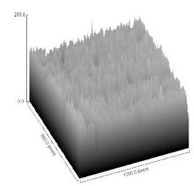	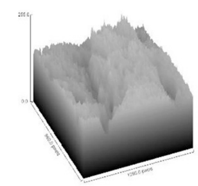	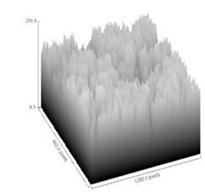
	Fractal dimension, FD (unit less)	2.884 ± 0.009^{a}	2.854 ± 0.010^{ab}	2.821 ± 0.007^{b}	2.771 ± 0.006^{c}	2.927 ± 0.005^{a}
	Surface openings, SO (%)	28.73 ± 1.33^{ab}	25.25 ± 1.57^{ab}	23.42 ± 2.02^{b}	8.76 ± 1.25^{c}	33.24 ± 1.28^{a}

Values are shown as mean ± standard deviation. "M" represents magnification. Bar scale in SEM micrograph represents 200 μm and 1 mm for the magnification of 500× and 100×, respectively. Lower-case letters (a-c) represent significant ($p < 0.05$) difference among means (within row). PC and PF represents pea protein concentrate and pea flour, respectively.

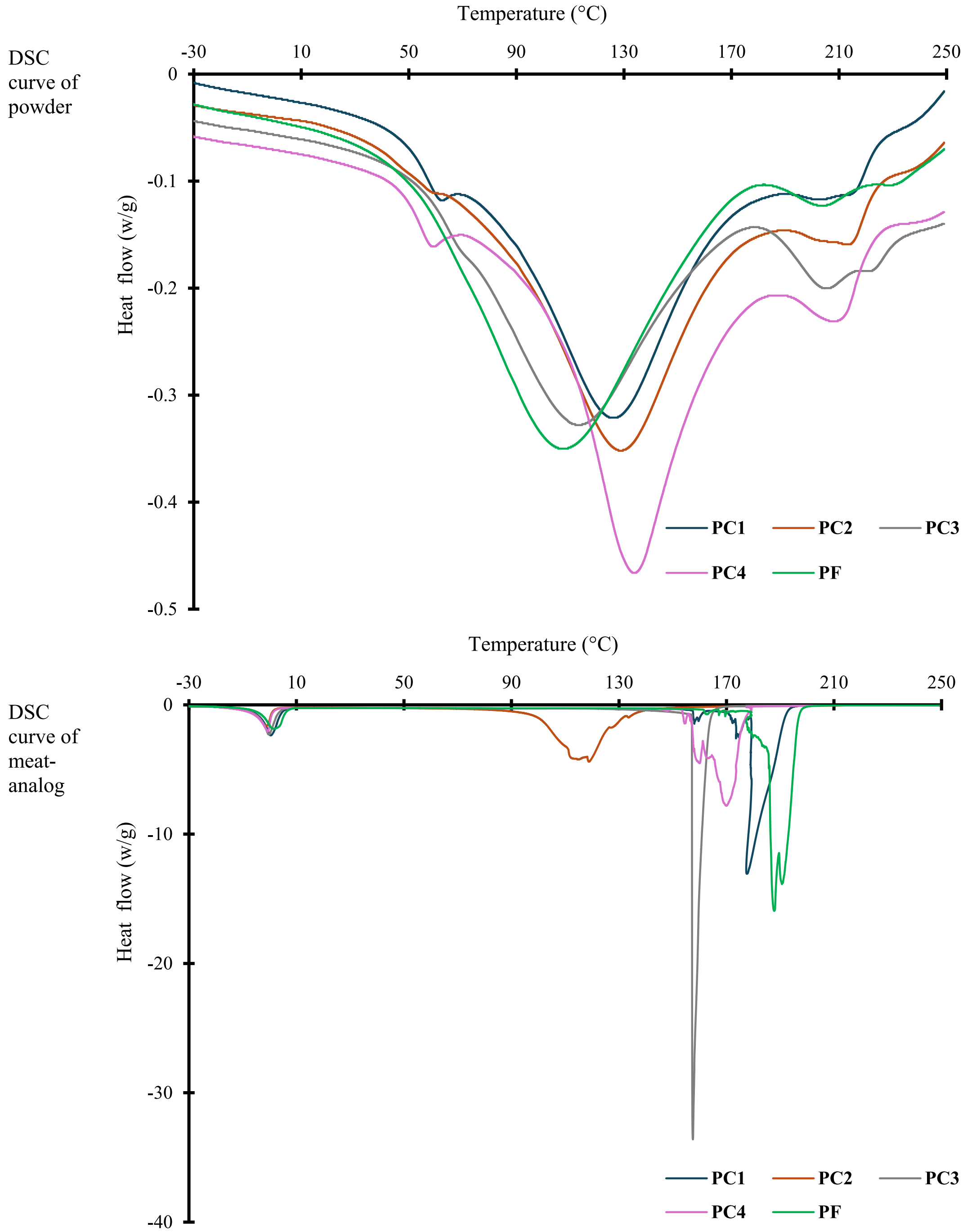

Fig. 2. Differential scanning calorimetry (DSC) curve of pea composites and meat-analogs.

Table 4
Thermal characteristics of pea composites and meat-analogs as evaluated by differential scanning calorimetry (DSC).

Sample type	Attribute	PC1	PC2	PC3	PC4	PF
Dry powder	1st peak onset (°C)	48.10 ± 1.02^{a}	50.20 ± 1.54^{a}	50.50 ± 1.63^{a}	51.20 ± 1.33^{a}	50.40 ± 1.34^{a}
	2nd peak onset (°C)	72.61 ± 0.88^{cd}	74.21 ± 0.98^{c}	83.61 ± 1.10^{b}	97.31 ± 1.21^{a}	70.21 ± 1.14^{d}
	2nd peak's peak (°C)	126.50 ± 2.12^{a}	130.40 ± 1.57^{a}	131.30 ± 1.88^{a}	134.12 ± 1.34^{a}	105.72 ± 1.21^{b}
	Enthalpy of 2nd peak (J/g)	175.82 ± 1.52^{bc}	177.61 ± 2.33^{b}	184.41 ± 5.45^{ab}	198.10 ± 2.35^{a}	167.30 ± 1.98^{c}
Meat-analog	1st peak onset (°C)	−4.40 ± 0.85^{a}	−4.10 ± 0.03^{a}	−4.1 ± 0.08^{a}	−5.31 ± 0.10^{a}	−3.80 ± 0.52^{a}
	2nd peak onset (°C)	154.11 ± 2.14^{ab}	103.41 ± 3.87^{c}	156.5 ± 2.11^{a}	161.20 ± 1.35^{a}	143.72 ± 3.54^{b}
	2nd peak's peak (°C)	157.70 ± 1.33^{bc}	166.80 ± 1.98^{ab}	177.8 ± 1.25^{a}	179.60 ± 10.10^{a}	144.51 ± 1.42^{c}
	Enthalpy of 2nd peak (J/g)	1211.31 ± 105.32^{b}	1235.72 ± 98.65^{ab}	1274.3 ± 125.15^{a}	1322.71 ± 185.65^{a}	1085.10 ± 115.42^{c}

Values are shown as mean ± standard deviation. Lower-case letters (a-c) represent significant ($p < 0.05$) difference among means (within row). PC and PF represents pea protein concentrate and pea flour, respectively.

temperature within the temperature ranges between 94.4 and 99.6 °C has been reported for chick pea composites (Yaputri et al., 2023). Wong et al. (2021) reported phase change temperature of 81.7 °C, 61.7 °C, and 59.8 °C for jackfruit seed starch, rice starch, and potato starch, respectively. Peak temperature ranged between 79.8 and 88.6 °C has been reported for lentils and beans (Xu et al., 2023).

However, in this study the DSC peak temperature of the 2nd broad peak was in the temperature range between 105.72 °C ± 1.21 and 134.12 °C ± 1.34. Ahmed et al. (2016) reported similar observation for lentil flours, linking to the melting of amylose-lipid complex components or protein denaturation in the flour samples. A similar amylose–lipid complex melting endotherm around 93–130.0 °C has been reported for lentil flours. A denaturization temperature within the range of 146–188 °C has been reported for plant-based protein substances (Webb et al., 2023). For the pea isolates the denaturization temperature ranged between 124.3 °C and 206.3 °C has been reported in literature (Asen & Aluko, 2022). The enthalpy (i.e., required heat energy to change the initial conformation of an existent system) for 2nd broad peaks were ranged between 167.30 J/g ± 1.98 and 198.10 J/g ± 2.35. Overall, the transition temperatures of the second endothermic peaks of pea composites as well as enthalpy varied substantially based on types (flour, concentrate) of the pea composites. Lower transition temperatures and enthalpies were observed for PF in comparison to PCs. According to Table 2, this could be attributed to lower protein and higher starch content of pea flour, in comparison to the studied pea protein concentrates. Proteins with largely ordered structures generally shows good thermal stability (represent as higher phase change/denaturization temperature) and protein molecules with more disulfide bonds may aid the protein's thermal stability (Shevkani et al., 2015). However, from a technological standpoint, pea composites with lower denaturation temperatures tend to consume the lower energy needed to change the protein conformation and consequently will have a cheaper processing cost (da Silva et al., 2021; Rodriguez & Beyrer, 2023).

The DSC curve of formulated MA samples exhibited two distinctive endothermic peaks. The first peak, very small in height and size appeared at low temperature range of −3.80 °C ± 0.52 and − 5.31 °C ± 0.10. The phase-transition at this low temperature zone may corresponds to ice-melting phenomenon (Bhuiyan & Ngadi, 2023a; Xue & Ngadi, 2007). However, the second broad peak was at a higher temperature zone with an onset temperature ranged between 103.41 °C ± 3.87 and 161.20 °C ± 1.35. The DSC peak temperature of the 2nd broad peak was in the temperature range of 144.51 °C ± 1.42 and 179.60 °C ± 10.10. The increase in protein content might had a positive correlation with the high hydrophobicity of protein, which could explain the observed high temperature of the pea protein concentrates. The enthalpy for 2nd broad peaks were ranges between 1085.10 J/g ± 115.42 and 1322.71 J/g ± 185.65. In comparison to pea flour (PF) based samples significantly higher enthalpy values were determined for pea concentrates-based samples. This could be linked to higher protein content of the PCs in comparison to PF. However, high enthalpy value of pea concentrates explained that they can withstand higher temperature before the change in their protein structure (Emkani et al., 2021), which indicates that their protein's structure is well-ordered in comparison to the protein's structure of pea flour. However, Rodriguez and Beyrer (2023) reported that presence of higher protein content in plant composites generally increase the energy requirement to make change in its initial state. However, enthalpies of the pea composites-based heat modulated MAs were incomparably higher than dry-powder of the corresponding pea composites. This is rationale, as the MA was prepared by applying intense heat, and under heat effect, intense protein denaturization were occurred. Hence, any subsequent change in protein conformations/structure required higher energy to undergo further changes in their denatured structure. This phenomenon had been reflected as a considerably higher onset temperature for the 2nd peak in the DSC curve of meat-analogs.

3.5. Chemical characteristics

Fig. 3 depicts fourier transformed infrared (FTIR) spectra and Table 5 summarizes chemical profile of pea composites and formulated MA as evaluated by FTIR spectra. The ATR-FTIR spectral pattern for all the studied samples (composites in powder form) looked very similar, since they were all originated from pea. However, there were differences in the intensities of the peaks at the absorption bands of the whole spectra. The IR absorption peaks at around 2922 cm^{-1} and 2852 cm^{-1} (asymmetrical and symmetrical stretching of —CH_2), 1743 cm^{-1} (C═O stretching), 1470 cm^{-1} (CH bending) and 1157 cm^{-1} (—C—O stretch; —CH_2 bending) of the spectra indicates the presence of oil/lipids (Bhuiyan & Ngadi, 2023b; Bhuiyan & Ngadi, 2024a; Rahman & Yu, 2017). A broad peak around 3000–3700 cm^{-1} region was due to the components of asymmetric and symmetric stretching modes of the H_2O molecule (Efimov et al., 2003; Nicolaisen, 2009). The IR spectra between 1700 and 1500 cm^{-1} represents amide I and amide II of the protein entity (Rahman & Yu, 2017; Reuben et al., 2014). The IR absorption bands for carbohydrates are generally in the range of 1191 cm^{-1} to 906 cm^{-1} (Reuben et al., 2014; Xin et al., 2013). Furthermore, relevant studies (Reuben et al., 2014; Xin et al., 2013; Yu, 2004) reported IR absorbance band for total carbohydrates in the range of 1180 cm^{-1} to 950 cm^{-1}, lignin (1510 cm^{-1}), and cellulosic materials (1295–1176 cm^{-1}). The differences in the absorbance peak characteristics (width, height) of different fried samples, represent the relative variation in concentrations.

From the FTIR spectra as well as estimated absorbance (a.u.) value it is evident that there were variations in chemical nature of the studied pea composites, as represented by different values for estimated moisture response (MR), protein response (PR), fat response (FR) and carbohydrate response (CR).The overall patter of FTIR spectra of the formulated meat-analogs looked quite similar. However, the differences in absorbance peaks (a.u.) are clearly noticeable. It ws observed that MR, FR and PR of the formulated MAs were substantially higher than the pea composites (as powder form). This is rationale, as water, canola oil and wheat gluten were externally added during the preparation of MA. From the estimated MR and PF values, it is apparent that higher moisture responses were observed for the samples whose protein response were higher. This indicates a positive correlation between protein content of pea composites and water retention in formulated MA. Overall, significantly higher PR and MR were observed for pea protein concentrates (PC4, PC3, PC2 & PC1) based meat-analogs in comparison to pea flour (PF) based meat-analog.

4. Conclusions

Techno-functional properties (water holding capacity, oil holding capacity, foaming capacity, foam stability, emulsion stability, least gelation concentration, solubility, etc.) of pea composites significantly impacted by protein content and particle size. The variations in techno-functional properties directly influences the characteristics of pea composites-based heat modulated meat analog (MA) formation. The optical properties, microstructural characteristics (surface plot, fractal dimension, surface openings), moldability, and acceptability of heat modulated MA were directly influenced by types of pea composites. Overall, protein content and particle size of pea composites paly crucial role on techno-functional properties of the composites that subsequently influenced the formation of heat-modulated MAs. Protein content and particle size of pea composites have also influenced the color and microstructure of heat-modulated MAs. MA formulated with pea flour showed better moldability and acceptability in comparison to pea concentrates. The results also highlighted that use of pea flour is a feasible option to produce heat modulated MA. The types of pea composites substantially impacted the thermal (denaturization temperature, enthalpy) and chemical features at their powder form as well as in the form of heat modulated meat analogs. The composition (predominantly

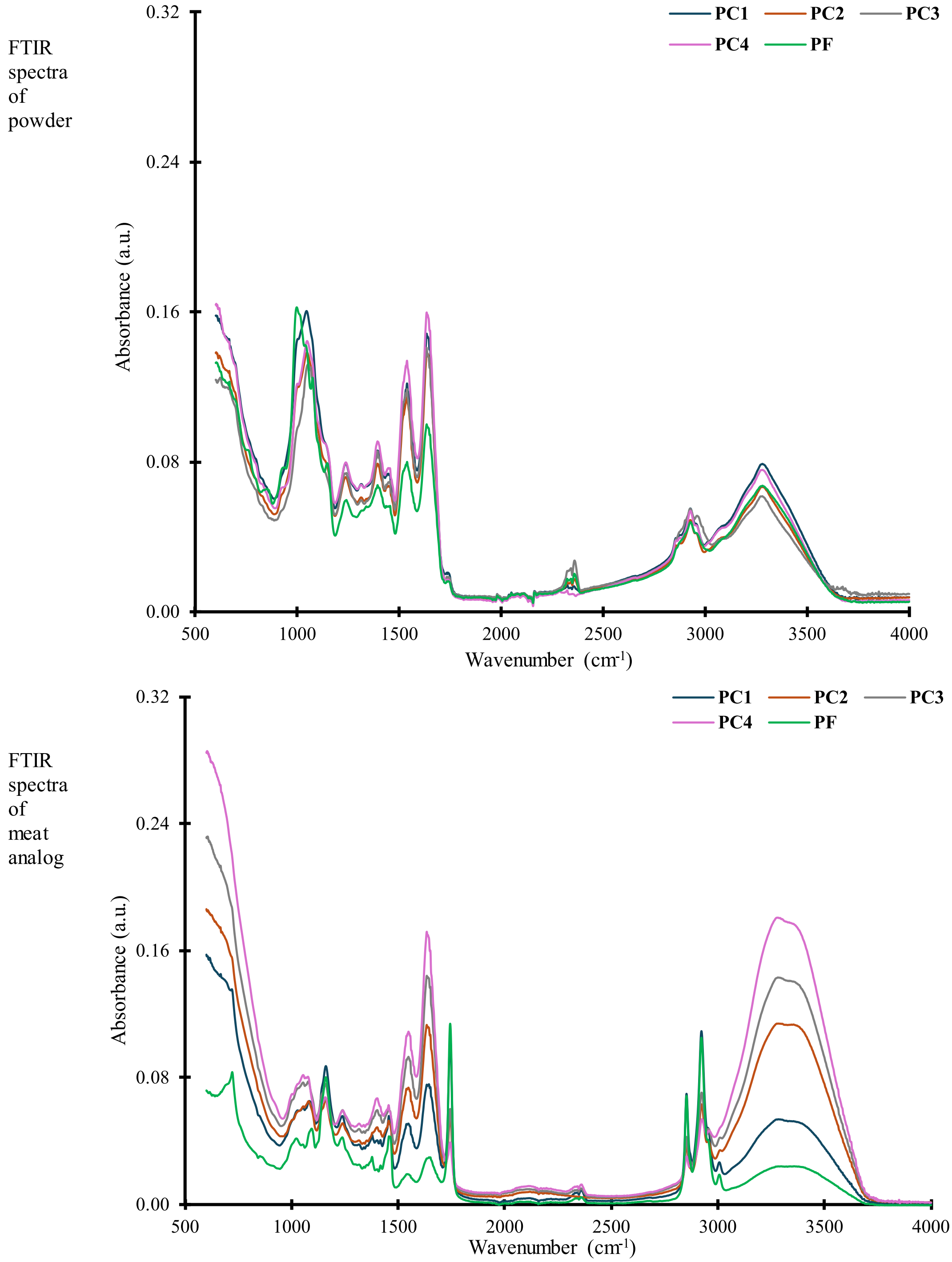

Fig. 3. The FTIR spectra of pea composites and meat-analogs.

the protein content) and particle size of pea composites plays crucial role in preparing plant proteins-based heat modulated MAs. Findings of this study would be useful in commercial production of pea composites-based MAs by employing novel heat-modulation technology. This study suggests more investigation (including diverse group of protein composites and various ingredients), to better understand and optimize the quality attributes of heat modulated meat analogs.

CRediT authorship contribution statement

Md. Hafizur Rahman Bhuiyan: Writing – review & editing, Writing – original draft, Visualization, Validation, Software, Methodology, Investigation, Formal analysis, Data curation, Conceptualization. **Laura Liu:** Formal analysis. **Anusha Samaranayaka:** Resources, Project administration, Funding acquisition. **Michael Ngadi:** Supervision, Resources, Project administration, Funding acquisition.

Declaration of competing interest

The authors declare that they have no known competing financial interests or personal relationships that could have appeared to influence the work reported in this paper.

Table 5
Chemical characteristics of pea composites and meat-analogs as evaluated by FTIR spectra.

Sample type	Absorbance (a.u.)	PC1	PC2	PC3	PC4	PF
Dry powder	Moisture response (MR)	21.90 ± 2.12[a]	18.12 ± 2.98[a]	18.92 ± 1.89[a]	19.22 ± 1.90[a]	17.30 ± 2.51[a]
	Protein response (PF)	5.71 ± 0.28[c]	8.61 ± 0.30[bc]	9.80 ± 0.22[b]	12.01 ± 0.35[a]	3.61 ± 0.12[d]
	Fat response (FR)	11.41 ± 1.05[a]	12.70 ± 1.33[a]	12.91 ± 0.08[a]	13.10 ± 1.14[a]	11.31 ± 1.23[a]
	Carbohydrate response (CR)	45.2 ± 1.251[a]	40.32 ± 2.74[a]	38.50 ± 1.25[b]	43.23 ± 1.85[a]	40.12 ± 2.42[ab]
Meat-analog	Moisture response (MR)	28.80 ± 1.02[c]	52.51 ± 1.33[b]	61.31 ± 1.52[b]	73.81 ± 2.31[a]	20.40 ± 1.24[d]
	Protein response (PR)	7.13 ± 0.08[cd]	9.60 ± 0.10[bc]	10.83 ± 0.09[b]	12.45 ± 0.08[a]	6.04 ± 0.09[d]
	Fat response (FR)	15.52 ± 1.85[a]	14.81 ± 1.96[a]	14.60 ± 1.66[a]	14.81 ± 1.34[a]	15.32 ± 1.48[a]
	Carbohydrate response (CR)	26.10 ± 0.12[b]	26.90 ± 0.23[b]	29.72 ± 0.88[a]	30.41 ± 0.85[a]	23.51 ± 0.98[c]

Values are shown as mean ± standard deviation. Lower-case letters (a-c) represent significant ($p < 0.05$) difference among means (within row). PC and PF represents pea protein concentrate and pea flour, respectively.

Data availability

Data will be made available on request.

Acknowledgements

Authors would like to appreciate the financial support of National Research Council Canada (NRC).

References

Abebe, W., Collar, C., & Ronda, F. (2015). Impact of variety type and particle size distribution on starch enzymatic hydrolysis and functional properties of tef flours. *Carbohydrate Polymers, 115*, 260–268.

Adenekan, M., Fadimu, G., Odunmbaku, L., & Oke, E. (2018). Effect of isolation techniques on the characteristics of pigeon pea (*Cajanus cajan*) protein isolates. *Food Science & Nutrition, 6*, 146–152.

Ahmed, J., Taher, A., Mulla, M. Z., Al-Hazza, A., & Luciano, G. (2016). Effect of sieve particle size on functional, thermal, rheological and pasting properties of Indian and Turkish lentil flour. *Journal of Food Engineering, 186*, 34–41. https://doi.org/10.1016/j.jfoodeng.2016.04.008

Aluko, R. E., Mofolasayo, O. A., & Watts, B. M. (2009). Emulsifying and foaming properties of commercial yellow pea (*Pisum sativum* L.) seed flours. *Journal of Agricultural and Food Chemistry, 57*, 9793–9800. https://doi.org/10.1021/jf902199x

Arteaga, V., Guardia, M., Muranyi, I., Eisner, P., & Schweiggert-Weisz, U. (2020). Effect of enzymatic hydrolysis on molecular weight distribution, techno-functional properties, and sensory perception of pea protein isolates. *Innovative Food Science & Emerging Technologies, 65*, Article 102449.

Asen, N., & Aluko, R. (2022). Physicochemical and functional properties of membrane-fractionated heat-induced pea protein aggregates. *Frontiers in Nutrition, 9*. https://doi.org/10.3389/fnut.2022.852225

Beniwal, A. S., Singh, J., Kaur, L., Hardacre, A., & Singh, H. (2021). Meat analogs: Protein restructuring during thermomechanical processing. *Comprehensive Reviews in Food Science and Food Safety, 20*(2), 1221–1249. https://doi.org/10.1111/1541-4337.12721

Bhuiyan, M. H. R., & Ngadi, M. (2023a). Electromagnetic, air and fat frying of plant protein-based batter-coated foods. *Foods, 12*(24). https://doi.org/10.3390/foods12244490

Bhuiyan, M. H. R., & Ngadi, M. (2023b). SR-FTIR microspectroscopy: Emerging 2D structural-chemical analytical technique for food quality and safety monitoring. *Food Bioscience, 56*(November), Article 103392. https://doi.org/10.1016/j.fbio.2023.103392

Bhuiyan, M. H. R., & Ngadi, M. (2024a). Post-fry oil distribution in batter coated fried foods. *LWT, 194*(January), Article 115819. https://doi.org/10.1016/j.lwt.2024.115819

Bhuiyan, M. H. R., & Ngadi, M. (2024b). Impact of batter solid-water ratio and frying time on meat-analog based coated fried food. *LWT - Food Science and Technology, 191* (September 2023), Article 115647. https://doi.org/10.1016/j.lwt.2023.115647

Bhuiyan, M. H. R., Yeasmen, N., & Ngadi, M. (2024a). Restructuring plant-derived composites towards the production of meat-analog based coated fried food. *Food Chemistry, 443*(August 2023), Article 138482. https://doi.org/10.1016/j.foodchem.2024.138482

Bhuiyan, M. H. R., Yeasmen, N., & Ngadi, M. O. (2024b). Multifractal analysis of meat-analog based coated fried foods texture profile. *Food Structure, 39*(August 2023), Article 100363. https://doi.org/10.1016/j.foostr.2023.100363

Boukid, F., Rosell, C. M., & Castellari, M. (2021). Pea protein ingredients: A mainstream ingredient to (re) formulate innovative foods and beverages. *Trends in Food Science & Technology, 110*, 729–742.

Chiang, J. H., Loveday, S. M., Hardacre, A. K., & Parker, M. E. (2019). Effects of soy protein to wheat gluten ratio on the physicochemical properties of extruded meat analogues. *Food Structure, 19*(November 2018), Article 100102. https://doi.org/10.1016/j. foostr.2018.11.002

Cruz-Solorio, A., Garın-Aguilar, M., Leal-Lara, H., Ramırez-Sotelo, M., & Valencia-del, T. (2014). Proximate composition of Pleurotus fruit body flour and protein concentrate. *Journal of Chemical, Biological and Physical Sciences, 5*, 52–60.

Deriu, A., Vela, A., & Ronda, F. (2022). Techno-functional and gelling properties of Acha (Fonio) (Digitaria exilis stapf) flour: A study of its potential as a new gluten-free starch source in industrial applications. *Foods, 11*(2), 183.

Du, S., Jiang, H., Yu, X., & Jane, J. (2014). Physicochemical and functional properties of whole legume flour. *LWT- Food Science and Technology, 55*(1), 308–313.

Efimov, A. M., Pogareva, V. G., & Shashkin, A. V. (2003). Water-related bands in the IR absorption spectra of silicate glasses. *Journal of Non-Crystalline Solids, 332*(1–3), 93–114.

Emkani, M., Oliete, B., & Saurel, R. (2021). Pea protein extraction assisted by lactic fermentation: Impact on protein profile and thermal properties. *Foods, 10*(3), 549.

Eze, C. R., Ekaette, I., & Ngadi, M.. Impact of ultra-centrifugal milling on the thermo-rheological, functional and physicochemical properties of yellow and green pea flour. https://ssrn.com/abstract=4687901.

Hong, S., Shen, Y., & Li, Y. (2022). Physicochemical and functional properties of texturized vegetable proteins and cooked patty textures: Comprehensive characterization and correlation analysis. *Foods, 11*(17). https://doi.org/10.3390/foods11172619

Hu, X., Zhou, H., & McClements, D. J. (2023). Impact of dispersion conditions and coacervation on fibril formation in gellan gum-potato protein mixtures. *Food Hydrocolloids, 145*(July), Article 109153. https://doi.org/10.1016/j.foodhyd.2023.109153

Ika, R. A., Yunianta, E., & T.. (2020). Characteristic of cowpea (vigna unguiculata) protein concentrates protein fraction on their solubility. *International Journal of ChemTech Research, 13*(1), 30–37.

Ivanova, P., Chalova, V., & Koleva, L. (2014). Functional properties of proteins isolated from industrially produced sunflower meal. *International Journal of Food Studies, 3* (2).

Karaca, A. C., Low, N., & Nickerson, M. (2011). Emulsifying properties of chickpea, faba bean, lentil and pea proteins produced by isoelectric precipitation and salt extraction. *Food Research International, 44*(9), 2742–2750.

Ladha-Sabur, A., Bakalis, S., Fryer, P. J., & Lopez-Quiroga, E. (2019). Mapping energy consumption in food manufacturing. *Trends in Food Science & Technology, 86*, 270–280.

Ma, K. K. (2020). *The comparison of functional and physical properties of commercial pulse proteins to soy protein*.

Maskus, H., Bourre, L., Fraser, S., Sarkar, A., & Malcolmson, L. (2016). Effects of grinding method on the compositional, physical, and functional properties of whole and split yellow pea flours. *Cereal Foods World, 61*(2), 59–64. https://doi.org/10.1094/CFW-61-2-0059

Mittal, S., Bhuiyan, M. H. R., & Ngadi, M. O. (2023). Challenges and prospects of plant-protein-based 3D printing. *Foods, 12*(21). https://doi.org/10.3390/foods12244490

Morr, C., German, B., Kinsella, J., Regenstein, J., Vanburen, J., Kilara, A., … Mangino, M. (1985). A collaborative study to develop a standardized food protein solubility procedure. *Journal of Food Science, 50*, 1715–1718.

Nicolaisen, F. M. (2009). IR absorption spectrum (4200-3100 cm-1) of H2O and (H2O)2 in CCl4. Estimates of the equilibrium constant and evidence that the atmospheric water absorption continuum is due to the water dimer. *Journal of Quantitative Spectroscopy and Radiative Transfer, 110*(18), 2060–2076.

Rahman, M. M., & Yu, P. (2017). Molecular basis of structural make-up of feeds in relation to nutrient absorption in ruminants, revealed with advanced molecular spectroscopy: A review on techniques and models. *Applied Spectroscopy Reviews, 52* (7), 653–673.

Reuben, S., Banas, K., Banas, A., & Swarup, S. (2014). Combination of synchrotron radiation-based Fourier transforms infrared microspectroscopy and confocal laser scanning microscopy to understand spatial heterogeneity in aquatic multispecies biofilms. *Water Research, 64*, 123–133.

Rodriguez, Y., & Beyrer, M. (2023). Impact of native pea proteins on the gelation properties of pea protein isolates. *Food Structure, 37*(March), Article 100340. https://doi.org/10.1016/j.foostr.2023.100340

Sahin, S., & Sumnu, G. (2006). Surface properties of foods. In S. Sahin, & S. G. Sumnu (Eds.), *Physical properties of foods* (pp. 229–248). New York: Springer. Food Science Text Series.

Sha, L., & Xiong, Y. L. (2020). Plant protein-based alternatives of reconstructed meat: Science, technology, and challenges. *Trends in Food Science and Technology, 102* (February), 51–61. https://doi.org/10.1016/j.tifs.2020.05.022

Shanthakumar, P., Klepacka, J., Bains, A., Chawla, P., Dhull, S., & Najda, A. (2022). The current situation of pea protein and its application in the food industry. *Molecules, 27* (16), 5354.

Shevkani, K., Singh, N., Kaur, A., & Rana, J. (2015). Structural and functional characterization of kidney bean and field pea protein isolates: A comparative study. *Food Hydrocolloids, 43*, 679–689.

da Silva, A., Almeida, F., & Sato, A. (2021). Functional characterization of commercial plant proteins and their application on stabilization of emulsions. *Journal of Food Engineering, 292*, Article 110277.

Sreerama, Y., Sashikala, V., Pratape, V., & Singh, V. (2012). Nutrients and antinutrients in cowpea and horse gram flours in comparison to chickpea flour: Evaluation of their flour functionality. *Food Chemistry, 131*, 462–468.

Wang, Q., Li, L., & Zheng, X. (2020). A review of milling damaged starch: Generation, measurement, functionality and its effect on starch-based food systems. *Food Chemistry, 15*(315), Article 126267. https://doi.org/10.1016/j.foodchem.2020.126267

Webb, D., Dogan, H., Li, Y., & Alavi, S. (2023). Physico-chemical properties and texturization of pea, wheat and soy proteins using extrusion and their application in plant-based meat. *Foods, 12*(8). https://doi.org/10.3390/foods12081586

Wong, K., Poh, G., Goh, K., Wee, M., & Jeyakumar, H. (2021). Comparison of physicochemical properties of jackfruit seed starch with potato and rice starches. *International Journal of Food Properties, 24*(1), 364–379.

Woo, H., Choi, M., Hahn, J., & Jin, Y. (2024). The technical potential of a sous-vide processing method for developing high-moisture textured soy protein. *Food Chemistry, 430*(March 2023), Article 136978. https://doi.org/10.1016/j.foodchem.2023.136978

Xia, S., Shen, S., Song, J., Li, K., Qin, X., Jiang, X., Xue, C., & Xue, Y. (2023). Physicochemical and structural properties of meat analogues from yeast and soy protein prepared via high-moisture extrusion. *Food Chemistry, 402*(February 2022). https://doi.org/10.1016/j.foodchem.2022.134265

Xin, H., Zhang, X., & Yu, P. (2013). Using synchrotron radiation-based infrared microspectroscopy to reveal microchemical structure characterization: Frost damaged wheat vs. normal wheat. *International Journal of Molecular Sciences, 14*(8), 16706–16718.

Xu, X., Tao, J., Wang, Q., Ge, J., Li, J., Gao, F., Gao, S., Yang, Q., Feng, B., & Gao, J. (2023). A comparative study: Functional, thermal and digestive properties of cereal and leguminous proteins in ten crop varieties. *LWT, 187*(May), Article 115288. https://doi.org/10.1016/j.lwt.2023.115288

Xue, J., & Ngadi, M. (2006). Rheological properties of batter systems formulated using different flour combinations. *Journal of Food Engineering, 77*(2), 334–341. https://doi.org/10.1016/j.jfoodeng.2005.06.039

Xue, J., & Ngadi, M. (2007). Thermal properties of batter systems formulated by combinations of different flours. *LWT- Food Science and Technology, 40*(8), 1459–1465. https://doi.org/10.1016/j.lwt.2006.02.007

Yaputri, B. P., Bu, F., & Ismail, B. P. (2023). *Salt solubilization coupled with membrane filtration-impact on the structure / function of chickpea compared to pea protein*.

Yu, P. (2004). Application of advanced synchrotron radiation-based fourier transform infrared (SR-FTIR) microspectroscopy to animal nutrition and feed science: A novel approach. *British Journal of Nutrition, 92*(6), 869.

Yuliarti, O., Kiat Kovis, T. J., & Yi, N. J. (2021). Structuring the meat analogue by using plant-based derived composites. *Journal of Food Engineering, 288*(January 2020), Article 110138. https://doi.org/10.1016/j.jfoodeng.2020.110138

Yuliarti, O., Ng, L., Koh, W. M., Abdullah Tan, M. F. B. M. F., & Dwi Sentana, A. (2023). Structural properties of meat analogue with added konjac gels. *Food Hydrocolloids, 142*(February 2022).